J. Fluid Mech. (1982), *vol.* 117, *pp.* 71–90
Printed in Great Britain

Numerical solutions for the spin-up of a stratified fluid

By JAE MIN HYUN, WILLIAM W. FOWLIS
N.A.S.A., Marshall Space Flight Center, Alabama 35812, U.S.A.
AND ALEX WARN-VARNAS
Naval Ocean Research and Development Activity,
Bay St Louis, Mississippi 39520, U.S.A.

(Received 23 March 1981 and in revised form 30 June 1981)

Numerical solutions for the impulsively started spin-up of a thermally stratified fluid in a cylinder with an insulating side wall are presented. Previous experimental and numerical work on stratified spin-up had not provided a comprehensive and accurate set of flow-field data. Further, comparisons of this work with theory showed, in general, a substantial discrepancy. The theory was scaled using the homogeneous meridional-flow spin-up time scale and thus viscous-diffusion effects were excluded from the interior. It was anticipated that these effects could only be significant on the larger viscous-diffusion time scale. However, the comparisons with theory showed a faster rate of decay for the measurements even over the shorter meridional-flow spin-up time scale. Previous workers had suggested a number of explanations but the cause of the discrepancy was still unresolved. To provide data to extend the previous work, a numerical model was used. The model was first checked against accurate experimental measurements of stratified spin-up made using a laser–Doppler velocimeter. New accurate results which cover ranges of Ekman number ($5{\cdot}92\times10^{-4} \leqslant E \leqslant 7{\cdot}24\times10^{-4}$), Rossby number ($0{\cdot}019 \leqslant \epsilon \leqslant 0{\cdot}220$), stratification parameter ($0{\cdot}0 \leqslant Sa^{-1} \leqslant 1{\cdot}03$), and Prandtl number ($5{\cdot}68 \leqslant \sigma \leqslant 7{\cdot}10$) are presented. These results show the radial and vertical structure of the decaying azimuthal and meridional flows. The inertial–internal gravity oscillations excited by the impulsive spin-up are clearly seen. By making use of conclusions from the previous work and the results presented in this paper, it is established that viscous diffusion in the interior is the cause of the discrepancy with theory. Stratification causes the meridional spin-up flow to be confined closer to the boundary disks. This results in non-uniform spin-up of the interior and hence flow gradients in the interior. These gradients introduce viscous diffusion into the interior sooner than anticipated by the theory. A previous suggestion that the faster decay rate is due to angular momentum being injected into the interior from an oscillation of the meridional corner-jet flow is shown to be untenable.

1. Introduction

Spin-up is the general process of adjustment of an initially uniformly rotating fluid to an externally imposed change in the magnitude of the rotation rate of its container. A review by Benton & Clark (1974) is available for this subject.

Recent work on spin-up dates from the linearized analysis of Greenspan & Howard

(1963), in which a homogeneous fluid contained between two infinite disks and rotating about an axis perpendicular to the disks is subjected to a small impulsive change in the rotation rate of the disks. Greenspan & Howard showed that the relative azimuthal flow created by a rotation-rate increase leads to the formation of Ekman layers on the boundary disks. These boundary layers exhibit an outward mass flux and draw fluid from the interior region (Ekman suction), which in turn leads to an inward meridional secondary circulation. This circulation fills the interior, where the direct effects of viscosity are negligible, and uniformly spins up the interior by angular-momentum advection and vortex-line stretching. For a rotation-rate decrease all the flow directions are reversed and the process is known as spin-down. Three distinct characteristic time scales are present in the solution: $O(\Omega^{-1})$, the time scale for the development of Ekman layers near the boundaries; $O(E^{-\frac{1}{2}}\Omega^{-1})$, the time for spin-up due to the meridional circulation; $O(E^{-1}\Omega^{-1})$, the viscous-diffusion time, where Ω is the rotation rate and E is the Ekman number.

More recently, Warn-Varnas *et al.* (1978) performed an extensive experimental and numerical investigation of the impulsive spin-up of a homogeneous fluid in a closed right-circular cylinder whose axis of symmetry is parallel to the rotation axis. The experimental part consists of azimuthal flow measurements made with a rotating laser–Doppler velocimeter (LDV). The rotating-LDV technique is capable of high accuracy with small space and time resolution, and disturbances of the flow are virtually negligible (Fowlis & Martin 1975). The numerical simulations used the Navier–Stokes equations in axisymmetric form and employed finite-difference techniques on a staggered mesh with variable grid spacings. A comparison of the experimental and numerical results showed excellent agreement, thus verifying the numerical model for that problem. Both the experimental and numerical techniques had sufficient resolution to exhibit clearly the weak inertial oscillations excited by the impulsive start.

The linearized, impulsively started spin-up of a stably stratified fluid in a cylinder was analysed theoretically by Walin (1969) and Sakurai (1969), resolving a controversy between the earlier works by Holton (1965) and Pedlosky (1967). The spin-up of a stratified fluid has characteristics which are different from homogeneous spin-up. The structure of the Ekman layers near the horizontal boundaries remains substantially unchanged, even for moderate stratification, but vertical motion is inhibited. Walin demonstrated that the outward Ekman mass flux enters into the interior directly from the corner regions. This flow is known as the corner jet. In the interior it forms a meridional secondary circulation that is restricted to a region closer to the Ekman layers. The weak oscillations excited by the impulsive spin-up are modified by the stratification, resulting in inertial–internal gravity modes. In the theory of Walin, the homogeneous meridional-flow spin-up time, $\tau = E^{-\frac{1}{2}}\Omega^{-1}$, was chosen to scale the equations. This choice of time scale removes from the theory processes occurring in time scales shorter and larger than τ. Thus the inertial–internal gravity modes, which occur in a time scale $O(\Omega^{-1})$, are not present in the solution and viscous-diffusion effects, which have a time scale $O(E^{-1}\Omega^{-1})$, are also absent.

In this paper previous experimental and numerical studies of stratified spin-up are described. The limitations of the previous work are discussed and the need for more, accurate, flow-field data is demonstrated. We decided to acquire such data using a numerical model. The model used by Warn-Varnas *et al.* (1978) was extended to allow for thermal stratification, and its predictions were checked by comparing them with the accurate experimental measurements of Lee (1975) obtained using a rotating LDV.

New results on the radial and vertical structures of the decaying azimuthal velocity over a range of Ekman number ($5{\cdot}92\times10^{-4} \leqslant E \leqslant 7{\cdot}24\times10^{-4}$), Rossby number ($0{\cdot}019 \leqslant \epsilon \leqslant 0{\cdot}220$), stratification parameter ($0{\cdot}0 \leqslant Sa^{-1} \leqslant 1{\cdot}03$) and Prandtl number ($5{\cdot}68 \leqslant \sigma \leqslant 7{\cdot}10$) are presented. Plots of the meridional stream function are also presented. We found, in agreement with previous workers, that, even over the time scale τ, the azimuthal flow decays faster than the predictions of the theory of Walin (1969). This discrepancy is discussed in the light of the previous work and the results presented in this paper.

2. Previous experimental and numerical work on stratified spin-up

Three carefully controlled laboratory experiments on impulsively started spin-up of a stratified liquid in a closed cylinder have been reported: Buzyna & Veronis (1971), Saunders & Beardsley (1975) and Lee (1975). In these experiments the plane boundaries were maintained horizontal and the rotation axis was vertical and coincident with the axis of symmetry of the cylinder. Buzyna & Veronis used a salt-stratified solution and photographed the movements of a neutrally buoyant dyed parcel of fluid to measure the angular displacements of the fluid. Saunders & Beardsley used a thermally stratified fluid and measured the perturbation temperature field with an array of thermistors. These authors compared their results with the linearized theory of Walin (1969). In order to do so they calculated variously defined spin-up times from their measurements. Details of these spin-up-time definitions and the comparison procedures are not essential for the discussion in this paper and so are not given. In general, these comparisons revealed that, even within the homogeneous meridional-flow spin-up time scale τ, the measured azimuthal velocities decay faster than those predicted by the theory, and the discrepancies in the decay rates are functions of the stratification parameter and the location in the fluid. Various causes such as the thermal variation of viscosity, probe drag and nonlinearity were postulated to account for the discrepancy.

Although the above experiments were carefully performed, the limitations of the measurement techniques meant that accurate flow-field data were not obtained. The relatively high-frequency, inertial–internal gravity modes were not detected because either the sampling times were large compared to the periods of the modes or the transducers were not sufficiently sensitive.

Lee (1975) used the disturbance-free, high-resolution, rotating-LDV technique to obtain quasicontinuous measurements of the azimuthal velocity in a thermally stratified spin-up flow. Lee also found that, in general, his results showed faster decay rates than the theory of Walin (1969), and this established that probe drag alone was not responsible for the discrepancy. Lee detected the oscillations excited by the impulsive start and showed that they were inertial–internal gravity modes. Lee compared his observed frequencies with the dispersion relation for axisymmetric, linearized, inviscid, inertial–internal gravity modes about a state of rigid rotation in a cylinder. This relation is

$$\beta = 2\Omega\left[\frac{1+(2\alpha_n/m\pi a)^2}{1+S^2(2\alpha_n/m\pi a)^2}\right]^{-\frac{1}{2}}, \tag{1}$$

where $a = R/H$, R is the radius, H is the half-depth of the cylinder, α_n are the zeros of the first-order Bessel function, m is any integer, and S is the stratification number (see § 3.2). The eigenfunctions of the problem are:

azimuthal velocity $\simeq J_1(\alpha_n r/R) \cos(m\pi z/H)$,

radial velocity $\simeq mJ_1(\alpha_n r/R) \cos(m\pi z/H)$,

vertical velocity $\simeq (\alpha_n/R) J_0(\alpha_n r/R) \sin(m\pi z/H)$.

Lee established that the dominant mode is given by $m = 2, n = 1$. This is as expected, since the impulsive change is an axisymmetric perturbation symmetrical about mid-depth and of the scale of the container. A similar result was found for the inertial modes in homogeneous spin-up (Fowlis & Martin 1975). Lee made no measurements of the meridional flow.

Numerical experiments on impulsively started, thermally stratified spin-up in a cylinder were conducted by Barcilon *et al.* (1975). These workers solved the Navier–Stokes equations in axisymmetric form by means of a finite-difference technique on a uniform grid. Azimuthal-flow results and meridional-stream-function plots were presented. Barcilon *et al.* again found that the model results decayed faster than the theory of Walin and they established, by comparing results for different values of the Rossby number, that the effects of nonlinearity were not the cause of the discrepancy.

The meridional-stream-function plots by Barcilon *et al.* showed the progressive confinement of the meridional circulation into the regions near the Ekman layers as the stratification increases. From an examination of these plots, Barcilon *et al.* pointed to an oscillation of the inclination of the corner jet between near-horizontal and near-vertical positions and they claimed a period of two or three times the rotation period for this oscillation. Barcilon *et al.* then argued that because of this oscillation of the corner jet some of the fluid spends more time in the viscous vertical boundary layer than it would if the jet were inclined at a steady angle to the vertical, as given by Walin's theory. While this fluid is within the vertical boundary layer, viscous shear adjusts its angular momentum to that of the side wall more efficiently than for interior fluid. Thus, according to Barcilon *et al.*, the fluid ejected into the interior from the vertical boundary layer yields its newly acquired angular momentum to the bulk of the interior, which then appears to have a faster spin-up time than predicted theoretically. In § 5, we point to a serious difficulty with this argument.

Barcilon *et al.* presented azimuthal-flow results for only a single location within the fluid. Although their results reveal clearly the inertial–internal gravity modes, no quantitative analysis of their properties was made.

3. The numerical model

To acquire more complete data to resolve the uncertainties still presented by the stratified spin-up problem we decided to use a numerical model. The model used by Warn-Varnas *et al.* (1978) for homogeneous spin-up was extended to include the energy equation and computations of the temperature fields. Before running the model routinely, its accuracy was established by comparing its predictions with the measurements of Lee (1975). A description of the model now follows.

Consider a right circular cylinder of radius R and height $2H$ filled with a fluid having kinematic viscosity ν, thermometric diffusivity κ, and coefficient of volumetric expansion α. These physical properties of the fluid are assumed to be constant. The top and bottom horizontal boundaries are thermal conductors and are kept at constant temperatures to produce a stable stratification. The vertical temperature difference is $2\Delta T$ over $2H$. The side-wall boundary is a thermal insulator. The initial flow is taken to be a solid-body rotation with angular velocity Ω_i and the rotation rate of the cylinder is changed impulsively to a new value $\Omega_f = \Omega_i + \Delta\Omega$. The Froude number $\Omega_f^2 H/g$ is much smaller than one (typically $O(10^{-3})$ in the present cases), and the effect of the Sweet–Eddington circulation will be ignored (Buzyna & Veronis 1971).

3.1. *Equations*

The governing equations are the axisymmetric incompressible Navier–Stokes equations for a Boussinesq fluid, written for rotating cylindrical co-ordinates (r,θ,z) with respective velocity components (u,v,w). Viewed in a frame rotating with the final rotation rate Ω_f, these equations are

$$\frac{\partial u}{\partial t} = -\frac{1}{r}\frac{\partial}{\partial r}(ru^2) - \frac{\partial}{\partial z}(uw) - \frac{1}{\rho_0}\frac{\partial p}{\partial r} + \left(2\Omega_f + \frac{v}{r}\right)v + \nu\left(\nabla^2 u - \frac{u}{r^2}\right), \tag{2}$$

$$\frac{\partial v}{\partial t} = -\frac{1}{r}\frac{\partial}{\partial r}(ruv) - \frac{\partial}{\partial z}(vw) - \left(2\Omega_f + \frac{v}{r}\right)u + \nu\left(\nabla^2 v - \frac{v}{r^2}\right), \tag{3}$$

$$\frac{\partial w}{\partial t} = -\frac{1}{r}\frac{\partial}{\partial r}(ruw) - \frac{\partial}{\partial z}(w^2) - \frac{1}{\rho_0}\frac{\partial p}{\partial z} + \alpha g T + \nu\nabla^2 w, \tag{4}$$

$$\frac{\partial T}{\partial t} = -\frac{1}{r}\frac{\partial}{\partial r}(ruT) - \frac{\partial}{\partial z}(wT) + \kappa\nabla^2 T, \tag{5}$$

$$\frac{1}{r}\frac{\partial}{\partial r}(ru) + \frac{\partial w}{\partial z} = 0, \tag{6}$$

where

$$\nabla^2 = \frac{1}{r}\frac{\partial}{\partial r}\left(r\frac{\partial}{\partial r}\right) + \frac{\partial^2}{\partial z^2},$$

p is the reduced pressure, T the temperature such that the full temperature equals $T_0 + T$, and the equation of state is

$$\rho = \rho_0(1-\alpha T), \tag{7}$$

in which T_0 and ρ_0 are the reference values of temperature and density, respectively.

The initial conditions for the fluid are

$$u = w = 0, \quad v = -\Delta\Omega r, \quad \frac{\partial T}{\partial z} = \frac{\Delta T}{H} \quad \text{at} \quad t = 0. \tag{8}$$

Clearly, the entire problem is symmetric about the mid-depth plane $z = 0$, and hence integration needs to be conducted for the bottom half of the cylinder, $-H \leqslant z \leqslant 0$, $0 \leqslant r \leqslant R$, only. The boundary conditions at the bottom disk are

$$u = v = w = 0, \quad T = -\Delta T \quad \text{at} \quad z = -H, \tag{9a}$$

and the symmetry conditions at the mid-plane are

$$\frac{\partial u}{\partial z} = \frac{\partial v}{\partial z} = w = 0, \quad T = 0 \quad \text{at} \quad z = 0. \tag{9b}$$

The boundary conditions on the cylinder wall are

$$u = v = w = 0, \quad \frac{\partial T}{\partial r} = 0 \quad \text{at} \quad r = R. \tag{10}$$

A thin solid cylinder of very small but finite radius ($r = r_i$) was inserted along the axis of symmetry to satisfy numerical stability requirements (Warn-Varnas *et al.* 1978). Symmetry conditions require that

$$u = v = \frac{\partial w}{\partial r} = 0, \quad \frac{\partial T}{\partial r} = 0 \quad \text{at} \quad r = r_i. \tag{11}$$

3.2. *Non-dimensional parameters*

The relevant non-dimensional parameters for the problem are defined as follows:

$\epsilon = \Delta\Omega/\Omega_i$, the Rossby number;

$E = \nu/4\Omega_i H^2$, the Ekman number;

$a = R/H$, the aspect ratio;

$F = \Omega_i H^2/g$, the Froude number;

$\sigma = \nu/\kappa$, the Prandtl number;

$S = N/2\Omega_i$, the stratification number;

where the Brunt–Väisälä frequency N is defined as $N = (\alpha g \Delta T/H)^{\frac{1}{2}}$. Note that the initial rotation rate Ω_i is chosen for the scaling.

3.3. *Numerical simulation technique*

Equations (2)–(6) and the initial and boundary conditions were finite-differenced on a staggered mesh with non-uniform grid spacings. The resulting time-dependent difference equations were solved by a time-marching procedure. Only a brief description is given here of the numerical techniques; for further details the reader is referred to the paper by Warn-Varnas *et al.* (1978).

The stretching of the grid was accomplished by use of the function

$$\xi = [\exp(r/r_l) - 1]/[\exp(r/r_l) + 1],$$

where r_l is a constant that controls the stretching of the boundary layers. A similar relationship was used in the z-direction. A 42×42 grid for the full domain was used and r_l was such that for the values of the Ekman numbers used there were about 8 points in each Ekman layer. The dependent variables were distributed over the staggered grid with the azimuthal velocity, temperature and pressure defined at the same grid points.

The pressure was found from a Poisson equation obtained by taking the divergence of (2) and (4). Thus

$$\frac{\partial D}{\partial t} = -\nabla^2 p + C, \tag{12}$$

where C denotes the combined divergence of the advection, Coriolis and buoyancy terms in the u- and w-equations, D is the divergence ($\nabla . \mathbf{u}$), which is small but, owing to machine round-off errors, not zero. This equation was solved by an ADI iterative approach. The optimum iteration parameters were calculated by the method outlined in Wachpress (1966 p. 194).

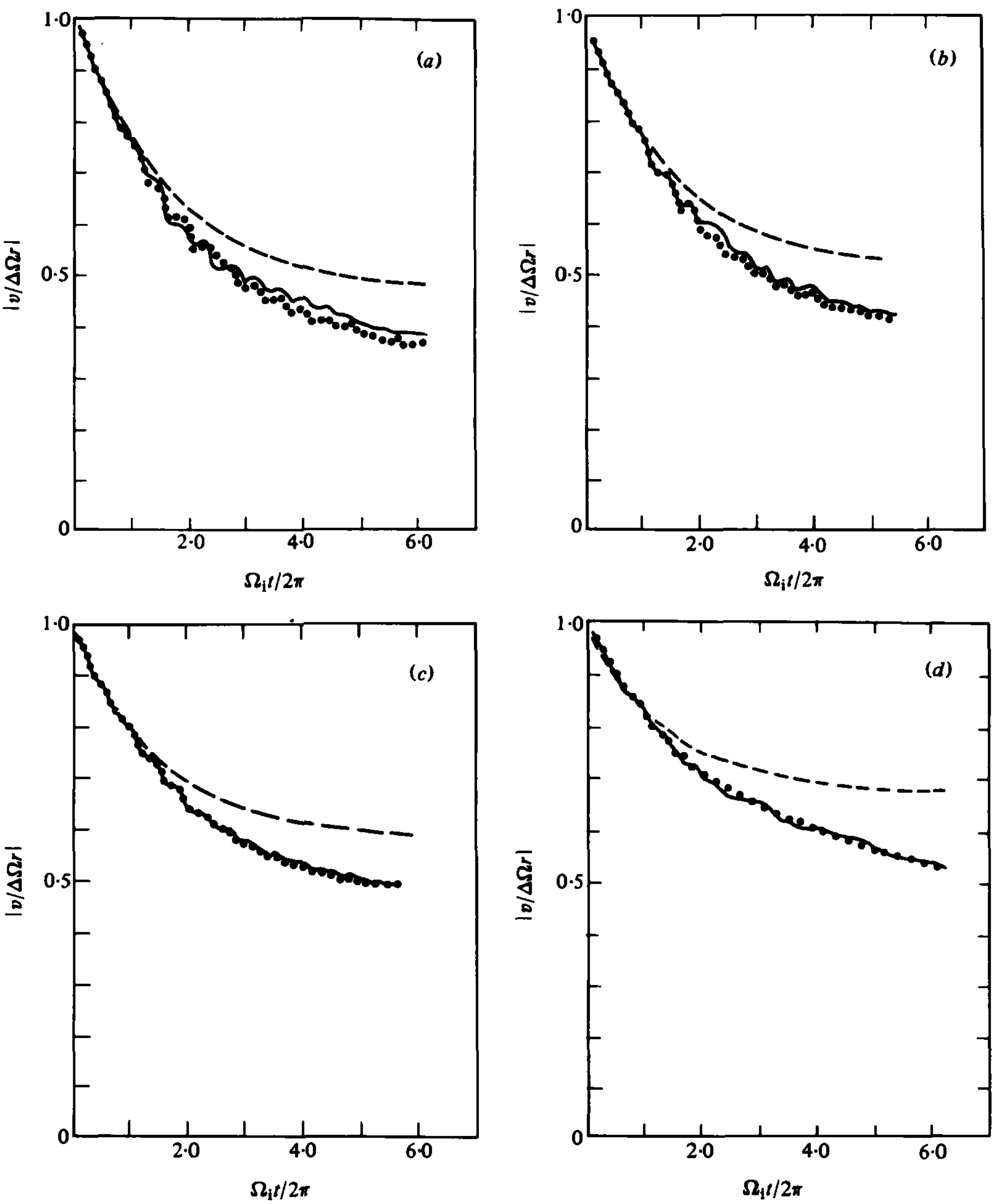

FIGURE 1. Comparison of spin-up results for $Sa^{-1} = 0{\cdot}49$. $E = 7{\cdot}24 \times 10^{-4}$, $\epsilon = 0{\cdot}222$. Dots are the laser measurements, solid lines the numerical results and broken lines the linear theoretical predictions. The vertical locations are at mid-depth ($z/H = 0{\cdot}00$) and the radial locations are (*a*) $r/R = 0{\cdot}30$, (*b*) 0·39, (*c*) 0·52, (*d*) 0·64.

3.4. *Verification of the numerical model*

The predictions of the numerical model were checked by comparing them with the accurate experimental measurements of Lee (1975). Lee's apparatus consisted of a cylindrical container (radius $R = 9{\cdot}50$ cm, height $2H = 6{\cdot}04$ cm) mounted on a

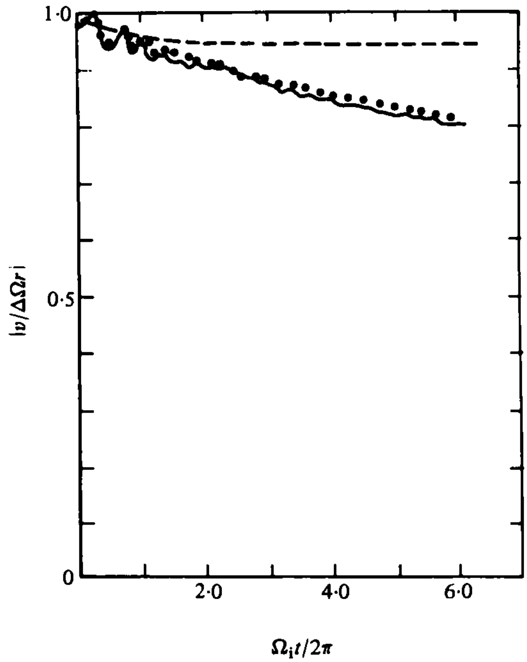

FIGURE 2. Comparison of spin-up results for $Sa^{-1} = 1{\cdot}03$, $E = 5{\cdot}92 \times 10^{-4}$, $\epsilon = 0{\cdot}222$. The location is at mid-radius, mid-depth ($r/R = 0{\cdot}5$, $z/H = 0{\cdot}00$).

precision-rate turntable with its axis of symmetry maintained vertical and made coincident with the rotation axis. The cylinder was of Plexiglas, and metal plates formed the upper and lower boundaries. The container was filled with water or methanol that was stably stratified by maintaining the upper boundary warmer than the lower boundary. This temperature difference $2\Delta T$ was 20 °C and a typical mean temperature of the fluid was 28 °C. The Plexiglas cylinder was further insulated by a layer of styrofoam and insulating tapes. Azimuthal flow measurements were made with a LDV system mounted on the turntable. This system is described in Lee (1975) and Fowlis & Martin (1975); it is capable of accurate, disturbance-free measurements of the relative flow. The spatial resolution was 0·05 cm in the radial direction and 0·0025 cm in the vertical direction and the temporal resolution was either 0·5 s or 1·0 s. The ranges of the non-dimensional parameters covered in Lee's experiments were $2{\cdot}43 \times 10^{-4} \leqslant E \leqslant 8{\cdot}75 \times 10^{-4}$, $0{\cdot}100 \leqslant \epsilon \leqslant 0{\cdot}222$, $0{\cdot}17 \leqslant Sa^{-1} \leqslant 1{\cdot}03$, $F \simeq O(10^{-3})$, and $\sigma \simeq 10$.

Results of the present numerical simulations were compared against corresponding data of Lee. Figures 1 and 2 are plots of scaled non-dimensional azimuthal velocity $|v/\Delta\Omega r|$ versus non-dimensional time $\Omega_i t/2\pi$ (i.e. the number of rotations based on Ω_i). The continuous curves are the numerical results and the dots are the experimental measurements of Lee. For later discussion, the theoretical predictions of Walin (1969), given in (13) (see § 5.1), are also included (broken curves) in figures 1 and 2.

The numerical simulations and the laboratory experiments were not performed for identical conditions; several small differences did exist. For the simulations the change in rotation rate was effectively instantaneous, but for the experiments there were small time delays due to the inertia of the turntable (Lee 1975). In the actual experi-

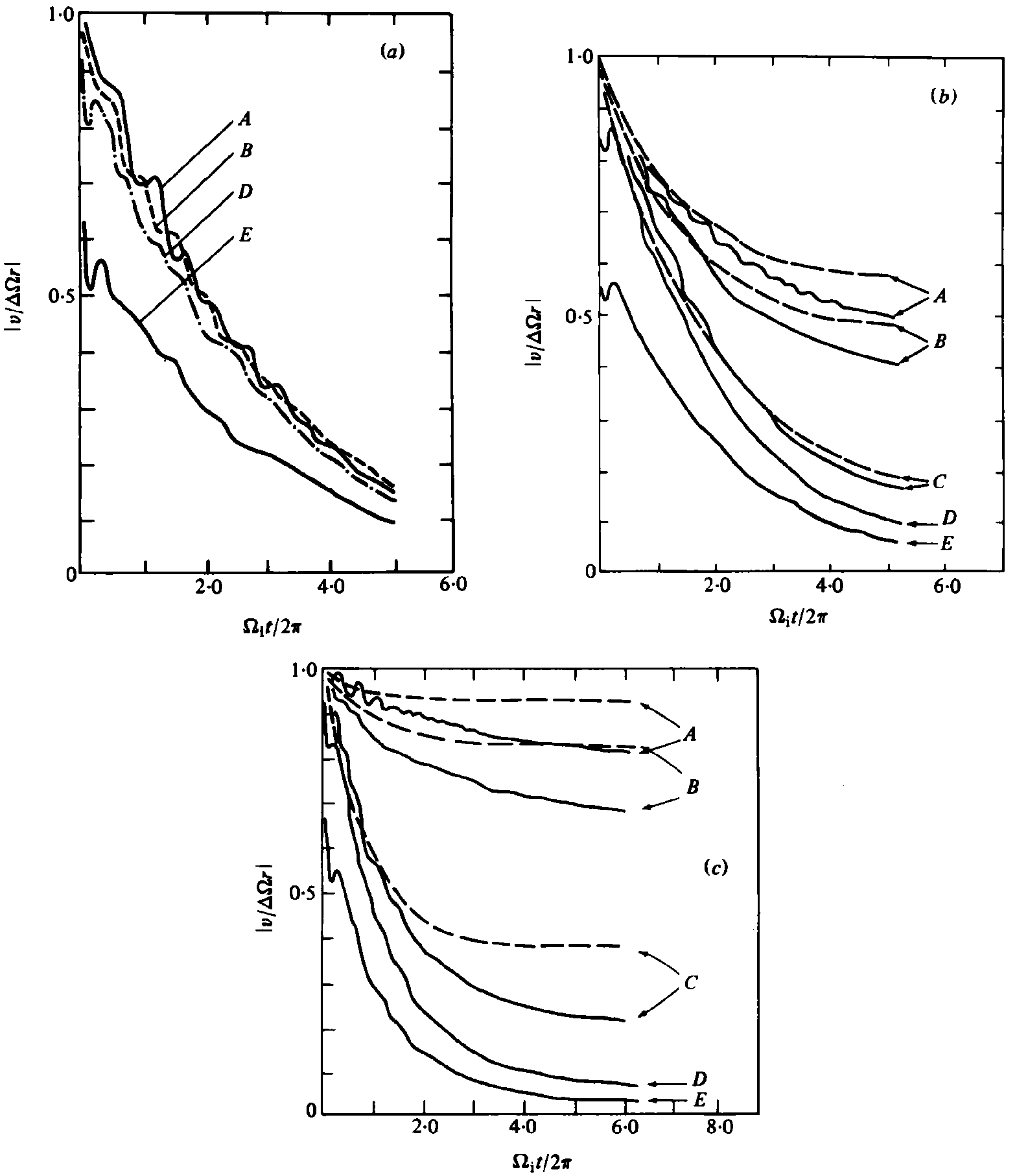

FIGURE 3. Spin-up results at mid-radius ($r/R = 0{\cdot}5$) for different stratification parameters: (*a*) $Sa^{-1} = 0$, (*b*) 0·49, (*c*) 1·03. Values of other parameters are listed in table 1. Vertical locations are (*A*) $z/H = 0$, (*B*) $-0{\cdot}42$, (*C*) $-0{\cdot}82$, (*D*) $-0{\cdot}93$, (*E*) $-0{\cdot}97$. The theoretical predictions for the interior points are shown in broken lines.

ments, the values of ν, κ and α have small variations over the depth of fluid because of the temperature difference, but in the simulations constant average values were adopted. The simulations were carried out with a small inner cylinder of radius $r_i = 0{\cdot}01$ cm (see §3, (11)). Warn-Varnas *et al.* (1978) showed that an increase of r_i to 0·1 cm made no difference to the results.

Figure number	Ω_i (rad s^{-1})	ϵ	E	Sa^{-1}	τ (s)
3(a), 4(a)	0·314	0·019	$7{\cdot}24\times10^{-4}$	0·0	118·3
3(b), 4(b)	0·314	0·019	$7{\cdot}24\times10^{-4}$	0·49	118·3
3(c), 4(c)	0·314	0·019	$5{\cdot}92\times10^{-4}$	1·03	130·8

TABLE 1. Values of the parameters for figures 3 and 4

Figure 1 shows the spin-up results for $Sa^{-1} = 0{\cdot}49$, $E = 7{\cdot}24\times10^{-4}$, $\epsilon = 0{\cdot}222$ ($\Omega_i = 0{\cdot}314$ rad s^{-1}, $\Omega_f = 0{\cdot}384$ rad s^{-1}) at four different radial locations at mid-depth ($z/H = 0$): (*a*) $r/R = 0{\cdot}30$ (SSU 38), (*b*) $r/R = 0{\cdot}39$ (SSU 37), (*c*) $r/R = 0{\cdot}52$ (SSU 35), (*d*) $r/R = 0{\cdot}64$ (SSU 36). The numbers in parentheses denote the run numbers used by Lee for his experiments. The fluid was water with $\nu = 8{\cdot}30\times10^{-3}$ cm^2 s^{-1}, $\kappa = 1{\cdot}46\times10^{-3}$ cm^2 s^{-1}, $\alpha = 2{\cdot}86\times10^{-4}$ °C^{-1}. The above quantities are stated to a significant number of digits only and this applies to all numbers in this paper based on measurement.

Figure 2 shows the spin-up results for $Sa^{-1} = 1{\cdot}03$, $E = 5{\cdot}92\times10^{-4}$, $\epsilon = 0{\cdot}222$ ($\Omega_i = 0{\cdot}314$ rad s^{-1}, $\Omega_f = 0{\cdot}384$ rad s^{-1}) at mid-radius ($r/R = 0{\cdot}5$) and mid-depth ($z/H = 0$) (SSU 71). The fluid was methanol with $\nu = 6{\cdot}79\times10^{-3}$ cm^2 s^{-1}, $\kappa = 9{\cdot}56\times10^{-4}$ cm^2 s^{-1}, $\alpha = 1{\cdot}28\times10^{-3}$ °C^{-1}.

Figures 1 and 2 show that the numerical and the experimental results agree to within a few per cent. The agreement is good not only for the overall decay of the azimuthal flow but also for the amplitudes and phases of the weakly excited, high-frequency, inertial–internal gravity modes. This agreement establishes the accuracy of the numerical model, and from this point on we proceeded to use the model to obtain new results. The agreement also shows that the small differences between the simulations and the experiments did not produce significant differences in the results. In particular, these comparisons establish that the variation of viscosity due to temperature in the laboratory experiments cannot be used to explain the observed discrepancy in spin-up rates between the theory and the previous experiments (see § 2).

4. Results

In this section the results of our numerical simulations of thermally stratified spin-up in a cylinder are presented. The dimensions of the cylinder are the same as those used in Lee's (1975) experiments (radius $R = 9{\cdot}50$ cm, half-depth $H = 3{\cdot}02$ cm, and the aspect ratio $a = R/H = 3{\cdot}14$). New results for both the azimuthal and meridional flow for different values of the stratification parameters are given.

4.1. *The spatial structure of the azimuthal flow*

Figure 3 shows the scaled non-dimensional azimuthal velocity $|v/\Delta\Omega r|$ at different vertical locations at mid-radius ($r/R = 0{\cdot}50$) for three values of the stratification parameter. The relevant parameters are listed in table 1.

Figure 3(*a*) shows the results for a homogeneous fluid. Curves (*A*) and (*B*) show

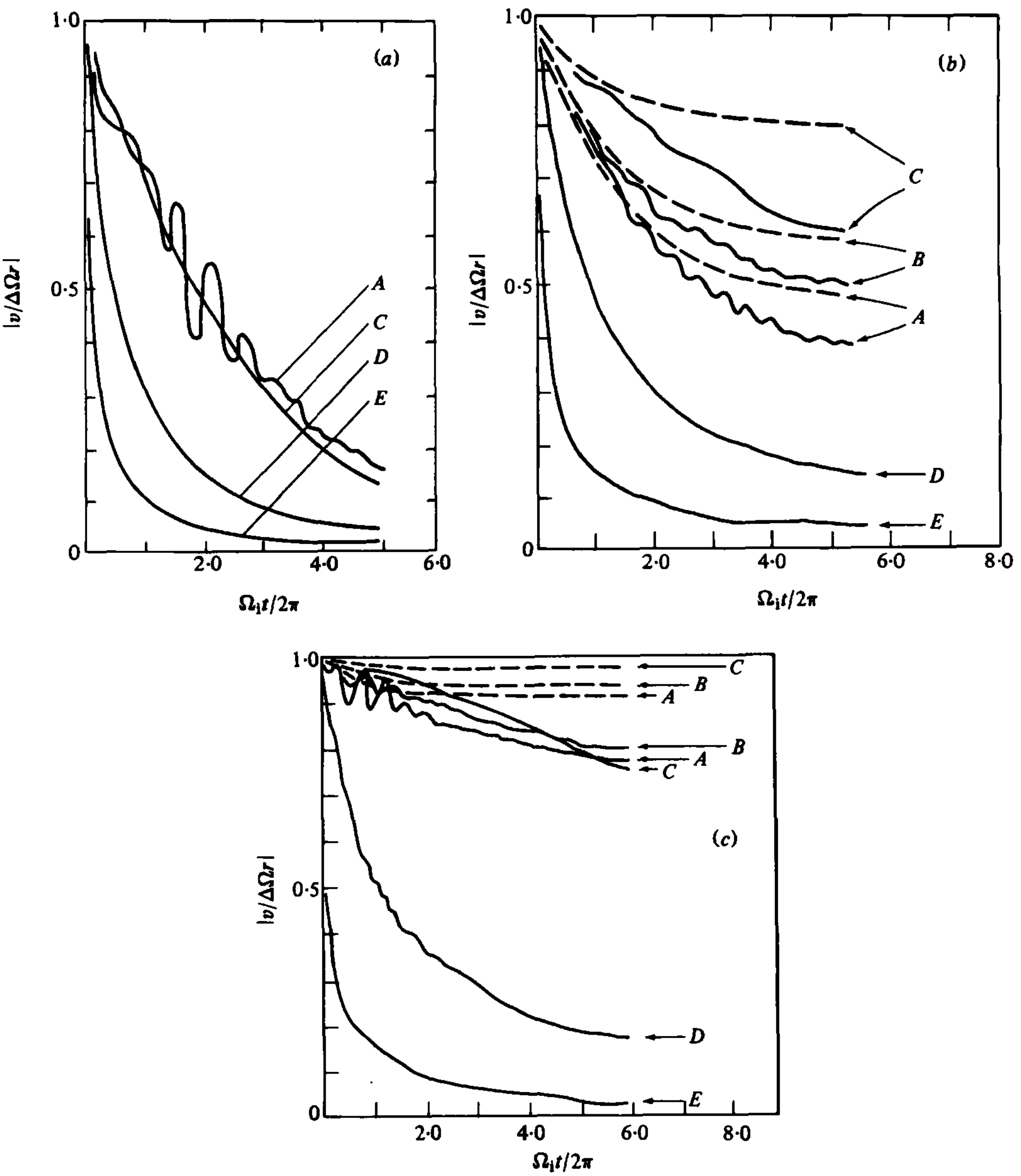

FIGURE 4. Spin-up results at mid-depth ($z/H = 0$) for different stratification parameters: (*a*) $Sa^{-1} = 0$, (*b*) 0·49, (*c*) 1·03. Values of other parameters are listed in table 1. Radial locations are (*A*) $r/R = 0{\cdot}23$, (*B*) 0·50, (*C*) 0·77, (*D*) 0·96, (*E*) 0·98. The theoretical predictions for the interior points are shown in broken lines.

that to substantial accuracy the interior azimuthal flow is uniform in the vertical direction. This is consistent with the Taylor–Proudman theorem. The horizontal Ekman boundary-layer thickness may be defined as $\delta_E \simeq E^{\frac{1}{2}}(2H)$, which for the parameters of figures 3 (*a*) and 3 (*b*) gives $\delta_E/H = 0{\cdot}054$ and for figure 3 (*c*) gives $\delta_E/H = 0{\cdot}049$. Therefore, curve (*D*) of figure 3 (*a*) is located slightly above the Ekman layer and the results show that down to this level the vertical uniformity of the azimuthal flow is still essentially valid. Curve (E) is within the Ekman layer and the velocity decays much faster in this viscous region than in the interior.

Figures 3(b, c) show the numerical results (solid lines) for a stratified fluid. For later discussion, the theoretical predictions of Walin (1969) for the interior points are also shown in broken lines. Clearly, the Taylor–Proudman theorem is no longer applicable; the interior azimuthal velocities are no longer uniform in the vertical direction. A comparison of curves (A) and (B) of figures 3(a, b, c) shows that in the interior, well away from the Ekman layers, the azimuthal flow decays initially at a slower rate as the stratification increases. On the other hand, curves (C) and (D) in figures 3(b, c) show that in the interior, close to the Ekman layers, the flow decays initially at a faster rate as the stratification increases. These results are interpreted as showing the effect of the progressive confinement of the meridional circulation by stratification (see §4.2). Note also from curves (C) in figures 3(b, c) that, although the meridional circulation spin-up phase proceeds more rapidly at this location for stronger stratification, it is less effective in the overall spin-up process. Finally, note from curves (E) in figure 3 that stratification enhances spin-up within the Ekman layer.

Figure 4 shows $|v/\Delta\Omega r|$ at different radial locations at mid-depth ($z/H = 0$) for three values of the stratification parameter. Walin's theoretical predictions for the interior points are shown in broken lines. The relevant parameters are listed in table 1.

Figure 4(a) shows the results for a homogeneous fluid. Curves (A) and (C) show that, apart from the inertial modes, the scaled azimuthal flow is uniform in the interior. Together with the results of figure 3(a) this implies solid-body rotation of the interior (Greenspan & Howard 1963). The side-wall boundary layer, which serves to adjust the azimuthal velocity to the wall, is of thickness $\delta_s \simeq E^{\frac{1}{4}}(2H)$, which for the parameters of figures 4(a, b) gives $\delta_s/H = 0{\cdot}33$ and for figure 4(c) gives $\delta_s/H = 0{\cdot}31$. Therefore the locations of curves (D) and (E) are within this viscous boundary layer, and at these locations spin-up proceeds much more rapidly.

Figures 4(b, c) show the results for a stratified fluid. The scaled azimuthal velocity is no longer uniform in the interior. In general, spin-up proceeds initially more rapidly at smaller radii and decreases as the radius increases until one reaches the viscous boundary layer on the outer wall. This result tells us that vortex-stretching by the meridional circulation is stronger at smaller radii. The results of figure 4(b) for moderate stratification ($Sa^{-1} = 0{\cdot}49$) display clearly this non-uniform stretching. The results of figure 4(c) for strong stratification ($Sa^{-1} = 1{\cdot}03$) show that in the interior at mid-depth the spin-up process is very weak. Curves (D) and (E) of figure 4 are for locations within the side-wall layer, and the velocity decays faster in this viscous region than in the interior; note, however, a trend toward a slower rate of decay for increasing stratification.

4.2. *The meridional flow*

Figures 5 and 6 show the plots of the meridional stream function from our numerical simulations for two values of the stratification parameter. Note the progressive confinement of the meridional circulation as the stratification increases. This result was predicted previously by Walin (1969) and demonstrated by Barcilon *et al.* (1975) in their numerical experiments.

Figure 5 shows the meridional-stream-function plots for the same parameters as the results shown in figures 3(b) and 4(b) ($Sa^{-1} = 0{\cdot}49$, $E = 7{\cdot}24 \times 10^{-4}$, $\epsilon = 0{\cdot}019$, $\Omega_i = 0{\cdot}314$ rad s^{-1}). The plots show a combination of the meridional circulation and

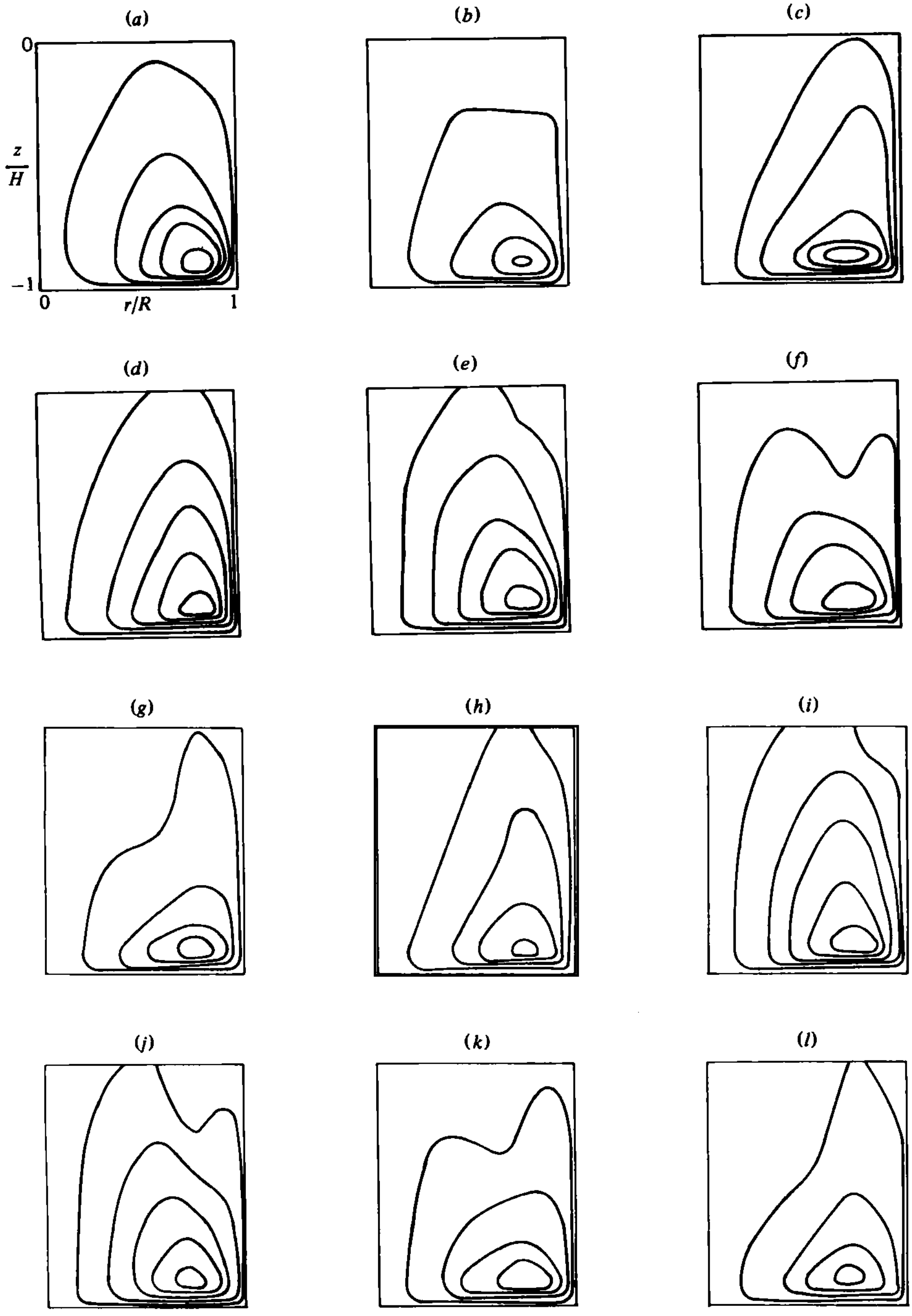

FIGURE 5. Meridional-stream-function contours for $Sa^{-1} = 0{\cdot}49$, $E = 7{\cdot}24 \times 10^{-4}$, $\epsilon = 0{\cdot}019$. (*a*) shows the contours 6 s (0·30 rotation periods) after the impulsive start, and (*b*)–(*l*) show the contours at 2 s (0·10 rotation periods) intervals thereafter.

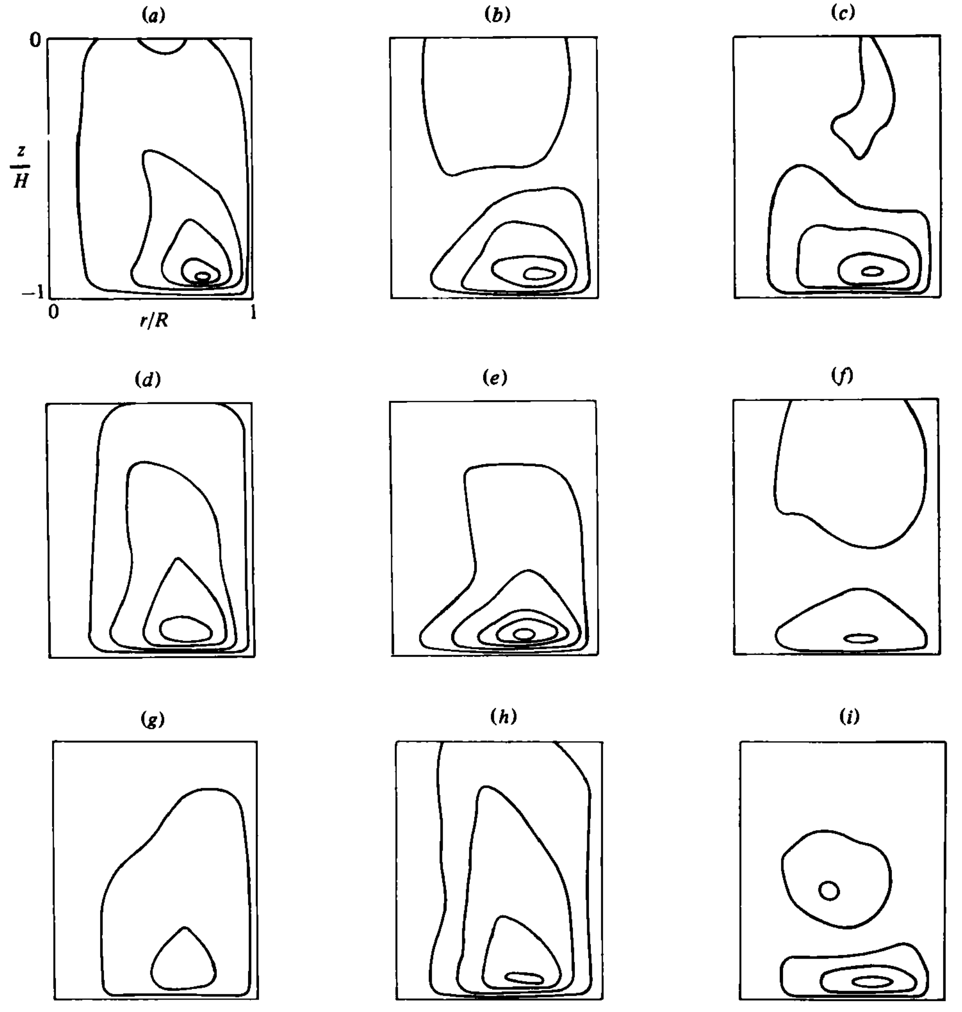

FIGURE 6. Meridional-stream-function contours for $Sa^{-1} = 1{\cdot}03$, $E = 5{\cdot}92 \times 10^{-4}$, $\epsilon = 0{\cdot}019$. (*a*) shows the contours 10 s (0·50 rotation periods) after the impulsive start, and (*b*)–(*i*) show the contours at 2 s (0·10 rotation periods) intervals thereafter.

the inertial–internal gravity modes. Using the azimuthal-velocity decay curve in figure 4 (*b*), the period of the inertial–internal gravity mode is found to be about 8·8 s, and thus about 2·5 periods of this oscillation are covered in figure 5. The period of the $m = 2$, $n = 1$ mode as calculated using (1) for the parameters of figure 5 and $\Omega_1 = 0{\cdot}314$ rad s^{-1} is 9·04 s. This agreement is consistent with the work of Lee (1975) (see § 2). Note also that the inclination of the corner jet is seen to oscillate with the period of the inertial–internal gravity modes. The velocities induced by the inertial–internal gravity modes and the velocities of the meridional circulation are comparable in magnitude. This is consistent with the results of Greenspan & Howard (1963) for the homogeneous problem. These workers found the velocities in the meridional circulation to be $O(E^{\frac{1}{2}}\epsilon\Omega R)$ and the velocities induced by the inertial modes also to be of the same order of magnitude, and this conclusion is not changed for the values of stratification considered in this paper.

Figure 6 shows the meridional-stream-function plots for the same parameters as the results shown in figures 3(*c*) and 4(*c*) ($Sa^{-1} = 1{\cdot}03$, $E = 5{\cdot}92 \times 10^{-4}$, $\epsilon = 0{\cdot}019$, $\Omega_1 = 0{\cdot}314$ rad s^{-1}). The same observations can be made as stated above for figure 5. Using the azimuthal velocity decay curves in figure 4(*c*), the period of the inertial–internal gravity mode is found to be about 6·8 s and thus about 2·5 periods of this oscillation are covered in figure 6. The period of the $m = 2$, $n = 1$ mode calculated using (1) for the parameters of figure 6 and for $\Omega_1 = 0{\cdot}314$ rad s^{-1} gives 6·55 s.

The plots of the interior azimuthal velocities in figures 3 and 4 reveal some characteristics of the inertial–internal gravity-mode structure. A comparison of curves (*A*) and (*B*) in figure 3 for fixed radius shows a reduced amplitude for the oscillations close to the quarter-depth location. This is consistent with $m = 2$ for the dominant mode, as was found by Lee (1975) (see § 2). A comparison of curves (*A*)–(*C*) in figure 4 for fixed depth shows the amplitude is relatively large at small radii compared with that at large radii. This result is not consistent with the simple inviscid eigenvalue problem stated in § 2. Warn-Varnas *et al.* (1978) found a similar discrepancy for the homogeneous-flow problem.

The radial velocity in the interior, which gives rise to the Coriolis term in the azimuthal velocity equation, is plotted in figure 7 as part of the diagnostic studies of (3) (see § 5.2). It is seen clearly that the radial velocity oscillates with the period of the dominant mode of the inertial–internal gravity oscillations.

5. Discussion of previous and present work

5.1. *Limitations of the theoretical models*

The excellent agreement obtained in comparisons between the results of the linearized theory of Greenspan & Howard (1963) and the experimental and numerical results for homogeneous spin-up (Warn-Varnas *et al.* 1978) demonstrates that the theory is quantitatively accurate. The solutions of Greenspan & Howard are for spin-up flow between two infinite disks, but they showed that the effect of the cylindrical side wall is small. This information, together with the high quality of the agreement out to almost two spin-up times, tells us that for homogeneous spin-up the interior is almost completely spun up by the meridional circulation alone. This is consistent with our picture of homogeneous spin-up occurring through an essentially solid-body rotation of the interior with direct viscous effects confined to boundary layers (see figures 3(*a*) and 4(*a*)). Further, Benton & Clark (1974) and Warn-Varnas *et al.* (1978) demonstrated that for $\epsilon \leqslant 0{\cdot}3$ only small departures from the results of linear theory occur.

A different picture emerges from the work of Walin (1969). In stratified spin-up, the effect of the meridional circulation, in general, is to bring about only a partial spin-up of the interior. Total adjustment to the final state of solid-body rotation at the new rotation rate is accomplished by viscous diffusion on the larger diffusion time scale $\tau_d = E^{-1}\Omega^{-1}$. However, comparisons to be discussed below between the theory of Walin and our numerical results show, in agreement with the previous experimental work (see § 2), substantial discrepancies for times of the order of the homogeneous meridional flow spin-up time $\tau = E^{-\frac{1}{2}}\Omega^{-1}$, which was the time scale of interest in Walin's analysis. For easy reference the linear expression ($\epsilon = 0$) derived by Walin for the decay of the azimuthal velocity in the interior is shown below in the form of the scaled non-dimensional azimuthal velocity:

$$\left|\frac{v}{\Delta\Omega r}\right| = 1+\frac{R}{ar}\sum_n C_n \frac{\cosh SK_n z/H}{\cosh SK_n} J_1(K_n ar/R)\,[1-\exp(-t/\tau_n)], \tag{13}$$

where $C_n = 2a/\alpha_n J_0(\alpha_n)$, $K_n = \alpha_n/a$, $\tau_n = E^{-\frac{1}{2}}\Omega^{-1}(\tanh SK_n)/SK_n$, and α_n are zeros of the first-order Bessel function.

Comparisons are made in figures 3(b, c), 4(b, c) of the theoretical predictions (broken lines) against the numerical results (solid lines) obtained for a very small Rossby number ($\epsilon = 0{\cdot}019$). Aside from the presence of the inertial–internal gravity modes (which were omitted from the theory), the overall disagreements between the theory and the numerical results are appreciable. In general, there is initial agreement for a time after the impulsive start, but the curves begin to diverge, with the numerical results decaying faster than the theory.

Comparisons are also made in figures 1 and 2 of the theoretical predictions (dashed lines) against the numerical results (solid lines) and the measurements (dots) of Lee (1975). It could be argued that these are unjustified comparisons since the theory is linear ($\epsilon = 0$) and the numerical results and the measurements are for $\epsilon = 0{\cdot}222$. A comparison of some of the numerical results in figures 1 and 2 for $\epsilon = 0{\cdot}222$ with the corresponding numerical results in figures 3 and 4 for $\epsilon = 0{\cdot}019$ shows differences of only a few per cent. (Compare figure 1(c) with curve (B) of figure 4(b), and figure 2 with curve (B) of figure 4(c).) Thus, over the range of ϵ studied, the results are only weakly dependent on ϵ, and hence nonlinearity cannot account for the discrepancies between the theory and the experiments. Barcilon *et al.* (1975) also reached this conclusion. The comparisons made in figures 1 and 2 show the same trends as those of figures 3 and 4.

Figure 3(b) shows comparisons of the theory with the numerical results for $Sa^{-1} = 0{\cdot}49$ for three different vertical locations at mid-radius. Curve (C) shows that the theory accurately predicts the flow in the interior regions close to the Ekman boundary layers. This is the region within which we know the meridional circulation is concentrated. Curves (B) and (A) show systematically increasing divergence of the results as higher levels approaching mid-depth are considered. We know that the meridional circulation weakens with height as we approach mid-depth. Figure 4(b) shows similar comparisons for three different radial locations at mid-depth. Note that we have systematically increasing divergences between the theory and numerical results as we move outward radially. We know that the spin-up effect of the meridional circulation is relatively strong for small radii at mid-depth.

Figures 3(c) and 4(c) show comparisons of the theory with the numerical results for $Sa^{-1} = 1{\cdot}03$ for the same vertical and radial locations as were used for figures 3(b) and 4(b). Although the discrepancies between the theoretical predictions and the numerical results are larger for the more strongly stratified case, the same general trends described for figures 3(b) and 4(b) are present.

5.2. *The effects of viscous diffusion in the interior*

The results presented in § 4.2 show that the corner jet oscillates with the period of the inertial–internal gravity mode. This oscillation was noticed previously by Barcilon *et al.* (1975), but these workers claimed to have observed a much larger period, i.e.

two or three rotation periods (see § 2). We suggest that the error arose from having too few stream-function plots, which in turn led to aliasing of the oscillation. More importantly, in order to account for the experimentally observed faster spin-up, Barcilon *et al.* then argued that this oscillating corner jet transports angular momentum from the vertical boundary layer into the bulk of the interior (see § 2). This argument presents a substantial difficulty. It has been shown (Greenspan 1969) that the inward radial distance moved by a fluid particle during the meridional circulation phase of spin-up is $O(\epsilon R)$, where ϵ is the Rossby number and R is the radius of the container. For the small-Rossby-number flows considered by Barcilon *et al.* this distance is small and hence the fluid ejected into the interior from the vertical boundary layer will not reach the bulk of the interior. The discussion given by Greenspan is for a homogeneous fluid, but the argument is not essentially changed for a stratified fluid.

The above comparisons show that agreement between the theory and the numerical results is good when we are dealing with locations and times for which the meridional-circulation flow is strong. Correspondingly, if this meridional flow is weak, agreement is poor. Thus, since viscous diffusion in the interior was omitted from the theory and since the possible effects of nonlinearity and other sources have been shown to be unimportant, it must be concluded that the observed discrepancy between the theory and the numerical results for the time span $\tau = E^{-\frac{1}{2}}\Omega^{-1}$ is due to viscous diffusion in the interior. The effects of viscous diffusion in the interior are enhanced for stratified spin-up over homogeneous spin-up since the effect of the meridional circulation in the stratified case is to produce radial and vertical gradients of the azimuthal velocity in the interior, whereas in the homogeneous case the azimuthal velocity in the interior decays essentially as solid-body rotation (see figures 3 and 4).

5.3. *Diagnostic studies of the azimuthal velocity equation*

The above conclusion concerning the viscous effects in the interior is verified by examining the size of each of the terms in the azimuthal-velocity equation. Among the terms on the right-hand side of (3), the nonlinear advective terms

$$-\frac{1}{r}\frac{\partial}{\partial r}(ruv), \quad -\frac{\partial}{\partial z}(vw),$$

and the curvature term $-vu/r$, are several orders of magnitude smaller than the Coriolis term, $-2\Omega_f u$, for the small-Rossby-number problems considered in this paper.

Figure 7 shows the plots of the Coriolis term (solid lines) $-2\Omega_f u$ and the viscous term (broken lines) $\nu(\nabla^2 v - v/r^2)$ as functions of time for up to $O(\tau)$. Hence, the solid line can be interpreted as the radial-velocity plot with the factor of $-2\Omega_f$ (see § 4.2).

Figure 7 (a) is for the homogeneous fluid at mid-radius, mid-depth using the same parameters as in figures 3 (a) and 4 (a). As anticipated, the viscous term is two or three orders of magnitude smaller than the Coriolis term. This is consistent with our earlier discussion on homogeneous spin-up that the azimuthal velocity in the interior decays essentially in solid-body rotation (see figures 3 (a) and 4 (a)) and that the viscous effects in the interior are negligible. Note in figure 7 (a) that the Coriolis term (or the radial velocity) oscillates with the period of the inertial mode.

Figure 7 (b) is for a stratified fluid ($Sa^{-1} = 1{\cdot}03$) at mid-radius and close to mid-depth ($r/R = 0$, $z/H = -0{\cdot}11$) using the same parameters as in figures 3 (c) and 4 (c). Notice that the Coriolis term (or the radial velocity) oscillates with the period of the

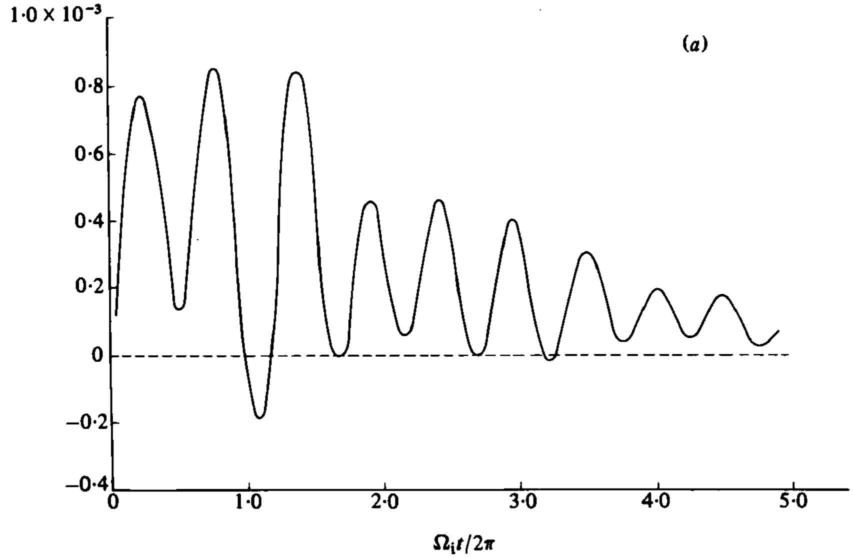

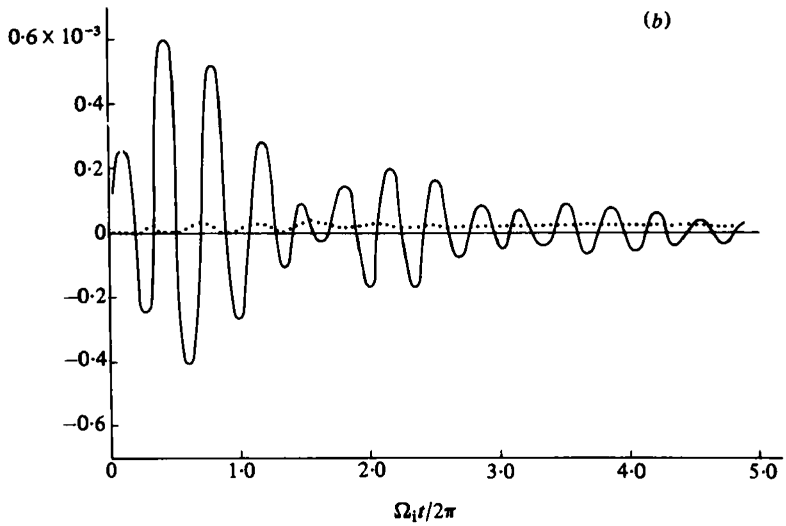

FIGURE 7. Plots of the Coriolis term (shown in solid lines) $-2\Omega_i u$, and the viscous term (shown in broken lines) $\nu(\nabla^2 v - v/r^2)$. The ordinate shows the values in c.g.s. units. (*a*) Results for homogeneous fluid at mid-radius, mid-depth. The values of the viscous term are $O(10^{-5}\text{–}10^{-6})$. (*b*) Results for $Sa^{-1} = 1{\cdot}03$ at $r/R = 0{\cdot}5$, $z/H = -0{\cdot}11$. (*c*) Results for $Sa^{-1} = 1{\cdot}03$ at $r/R = 0{\cdot}5$, $z/H = -0{\cdot}78$.

inertial–internal gravity mode (see § 4.2). Since the theory of Walin (1969) filtered out the inertial–internal gravity modes, the Coriolis term used in Walin's formulation would be obtained by averaging the Coriolis term shown in the figure over one period of the inertial–internal gravity oscillation. We also noted that in stratified spin-up substantial flow gradients are developed in the interior, which give rise to enhanced viscous diffusion. It is obvious in figure 7 (*b*) that at mid-radius and near mid-depth this averaged Coriolis term is larger than the viscous term for early times, but after about 1 rotation period the averaged Coriolis term becomes comparable to or even

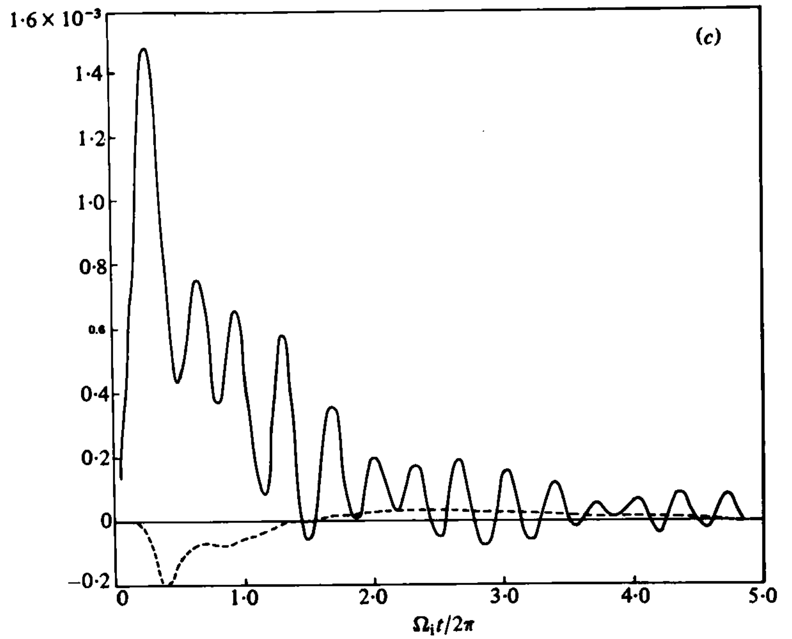

FIGURE 7(c). For legend see p. 88.

smaller than the viscous term. Therefore, omitting the viscous term and retaining only the averaged Coriolis term, as was done in Walin's theory, would lead to an appreciable underestimation of the acceleration of fluid in the azimuthal direction (see curve (A) of figure 3(c)).

Figure 7(c) is the same as figure 7(b), except that the location ($r/R = 0·5, z/H = -0·78$) is closer to the Ekman layer. We know that the meridional circulation is concentrated in this region, and figure 7(c) shows that the Coriolis term is generally larger at this level than near mid-depth as shown in figure 7(b). It is also apparent in figure 7(c) that the viscous term becomes comparable to the averaged Coriolis term after about 2·5 rotation periods. Consequently, at this level the theoretical prediction is expected to diverge from the numerical results after a longer period of time has elapsed (compare curve (C) with curve (A) of figure 3(c)).

It has now been established that the source of the discrepancy between theory and the numerical results in stratified spin-up is the neglect in the theory of viscous diffusion in the interior over the time scale τ.

6. Conclusions

The spin-up flow of a thermally stratified fluid in a cylinder with an insulating side wall has been examined numerically using the model of Warn-Varnas *et al.* (1978). The numerical results were first checked by comparing them against the accurate laser–Doppler measurements of Lee (1975), and excellent agreement was obtained. New results on the radial and vertical structures of the decaying azimuthal flow were presented. It was shown that substantial flow gradients are created in the interior of the fluid during the meridional-circulation spin-up phase. We found, in agreement with previous workers, that over the time scale τ the azimuthal flow decayed significantly faster than the predictions of the theory of Walin (1969). By making use of established conclusions from previous work and the results presented in this paper it has been established that viscous diffusion in the interior, arising from the interior-flow gradients, is the cause of the discrepancy with the theory.

Plots of the meridional stream function show a combination of the meridional-circulation flow and the inertial–internal gravity oscillations excited by the impulsive spin-up. A comparison of the period and spatial structure of these oscillations with the results of a simple eigenvalue problem indicated that most of the energy is in the axisymmetric $m = 2$, $n = 1$ mode. An oscillation of the corner jet was shown to be the result of the superposition of the meridional-circulation flow and the inertial–internal gravity modes. The suggestion by Barcilon *et al.* (1975) that this oscillating corner jet is responsible for the faster decay of the azimuthal flow is shown to be untenable.

J.M.H. is indebted to the National Research Council for the Senior Postdoctoral Research Associateship he held during the performance of this investigation. The Associateship and the research were supported by the Global Weather Program of the Office of Space and Terrestrial Applications, N.A.S.A. Headquarters.

REFERENCES

BARCILON, A., LAU, J., PIACSEK, S. & WARN-VARNAS, A. 1975 Numerical experiments on stratified spin-up. *Geophys. Fluid Dyn.* **7**, 29.

BENTON, E. R. & CLARK, A. 1974 Spin-up. *Ann. Rev. Fluid Mech.* **6**, 257.

BUZYNA, G. & VERONIS, G. 1971 Spin-up of a stratified fluid. *J. Fluid Mech.* **50**, 579.

FOWLIS, W. W. & MARTIN, P. J. 1975 A rotating laser Doppler velocimeter and some new results on the spin-up experiment. *Geophys. Fluid Dyn.* **7**, 67.

GREENSPAN, H. P. 1969 *The Theory of Rotating Fluids*. Cambridge University Press.

GREENSPAN, H. P. & HOWARD, L. N. 1963 On a time-dependent motion of a rotating fluid. *J. Fluid Mech.* **17**, 385.

HOLTON, J. R. 1965 The influence of viscous boundary layers on transient motions in a stratified rotating fluid. *J. Atmos. Sci.* **22**, 402.

LEE, S. M. 1975 An investigation of stratified spin-up using a rotating laser–Doppler velocimeter. M.S. thesis, Florida State University.

PEDLOSKY, J. 1967 The spin-up of a stratified fluid. *J. Fluid Mech.* **28**, 463.

SAKURAI, T. 1969 Spin-down problem of rotating stratified fluid in thermally insulated circular cylinders. *J. Fluid Mech.* **37**, 689.

SAUNDERS, K. D. & BEARDSLEY, R. C. 1975 An experimental study of the spin-up of a thermally stratified rotating fluid. *Geophys. Fluid Dyn.* **7**, 1.

WACHPRESS, E. L. 1966 *Iterative Solutions of Elliptic Systems*. Prentice-Hall.

WALIN, G. 1969 Some aspects of time-dependent motion of a stratified rotating fluid. *J. Fluid Mech.* **36**, 289.

WARN-VARNAS, A., FOWLIS, W. W., PIACSEK, S. & LEE, S. M. 1978 Numerical solutions and laser–Doppler measurements of spin-up. *J. Fluid Mech.* **85**, 609.